

Observation and simulation of all angular magnetoresistance oscillation effects in the quasi-one-dimensional organic conductor (DMET)(2)I-3

Authors: Pashupati Dhakal, Harukazu Yoshino, Jeong Il Oh, Koichi Kikuchi, Michael Naughton

Persistent link: <http://hdl.handle.net/2345/3341>

This work is posted on [eScholarship@BC](#),
Boston College University Libraries.

Published in *Physical Review Letters*, vol. 105, no. 6, August 2010

Copyright (2010) by The American Physical Society. These materials are made available for use in research, teaching and private study, pursuant to U.S. Copyright Law. The user must assume full responsibility for any use of the materials, including but not limited to, infringement of copyright and publication rights of reproduced materials. Any materials used for academic research or otherwise should be fully credited with the source.

Observation and Simulation of All Angular Magnetoresistance Oscillation Effects in the Quasi-One-Dimensional Organic Conductor (DMET)₂I₃

Pashupati Dhakal,¹ Harukazu Yoshino,² Jeong Il Oh,¹ Koichi Kikuchi,³ and Michael J. Naughton¹

¹*Department of Physics, Boston College, Chestnut Hill, Massachusetts 02467, USA*

²*Graduate School of Science, Osaka City University, Osaka 558-8585, Japan*

³*Graduate School of Science, Tokyo Metropolitan University, Tokyo 192-0397, Japan*

(Received 26 March 2010; published 2 August 2010)

Measurements and calculations of magnetotransport in the organic conductor (DMET)₂I₃ detect and simulate all angular magnetoresistance oscillations known for quasi-one-dimensional conductors. By employing the actual triclinic crystal structure in the calculations, these results address the putative vanishing of the primary magnetoresistance phenomenon, the Lebed magic angle effect, for orientations in which it was expected to be strongest. They also show a common origin for Lebed and the so-called Lee-Naughton oscillations and confirm the generalized nature of angular effects in such systems.

DOI: 10.1103/PhysRevLett.105.067201

PACS numbers: 75.47.-m, 73.43.Qt, 74.70.Kn

Quasi-one-dimensional (Q1D) molecular conductors are highly anisotropic materials which show remarkable oscillatory magnetotransport phenomena with respect to crystal orientation in a strong magnetic field [1,2]. Several types of angular magnetoresistance oscillations (AMRO) have been observed in Q1D conductors. In the prototypical Q1D conductors based on the TMTSF molecule, Lebed “magic angle” (LMA) resonances [3–7], Danner-Kang-Chaikin (DKC) oscillations [8,9], and the Yoshino angular effect (YAE) [10–12] have been observed for field rotations about the three principle axes. In addition, more complex Lee-Naughton (LN) oscillations [13] were observed when the magnetic field was rotated through arbitrary, out-of-plane directions [12–14].

While such AMRO effects have been detected in several Q1D materials, their origin(s) and relationships to each other have intrigued researchers for over two decades. For example, while numerical calculations of magnetoconductivity using the Boltzmann transport equation for a Q1D system qualitatively reproduce the observed AMRO [10], several other theoretical models introduced to explain interlayer AMRO in Q1D systems, quasiclassical and quantum [15–24], qualitatively explain only some of the observed effects (DKC, YAE, and LN). Curiously, these theories have consistently failed to simulate the initially predicted [3,4], and detected [5,6], Lebed effect. The models in Refs. [21–23] result in identical expressions for the interlayer conductivity, though from slightly different starting assumptions, each yielding a series of resistivity minima for integer values of an index n in the Lebed relation $\tan\theta = nb/c$, where θ is the magnetic field angle between lattice directions b and c .

According to these models, each n th-order oscillation is modulated by an equivalent order Bessel function that is itself a function of the magnetic field ratio B_x/B_z , x and z being the intrachain and interplane (the most and least conducting) directions, respectively. However, when the field is rotated in the y - z plane (i.e., perpendicular to the

Q1D chains x), the presumed optimal situation for the Lebed effect, all Bessel functions vanish, with the exception of $n = 0$, and the resulting resistivity has a smooth, featureless angular variation with field, with *no* Lebed oscillations. In spite of this fact, the Lebed effect was recently suggested to be the “only fundamental angular effect” [25], with all others (DKC, YAE, and LN) being modulations of it. This seems arguable since, experimentally, Lebed oscillation amplitudes have been anecdotally observed to *decrease* (some becoming immeasurably small) as the field rotation plane approaches the “preferred” y - z plane where, again, the effect is expected to be *strongest* [12,25].

To date, all available theoretical models [15–26] have employed an orthorhombic or cubic approximation to the actual triclinic crystal structure of the materials in which the AMRO effects have been seen. In this work, we have simulated conductivity via numerical calculations that employ the *actual* triclinic lattice parameters of a Q1D conductor, (DMET)₂I₃, and measured its interlayer magnetoresistance. We show that all AMRO effects appear in both theory and experiment and, moreover, now match in the Lebed rotation plane with respect to the overall magnetoresistance and the presence of LMA features, including their still somewhat curious diminishment upon approaching the y - z plane.

(DMET)₂I₃ [27] shares many similarities with the TMTSF system, including Q1D AMRO effects, superconductivity, and a triclinic crystal structure. In this symmetry, the orthogonal set (x, y, z) is represented by (b, a', c^*) , based on the lattice parameters b , a , and c [11]. While the aforementioned AMRO effects have all been detected in (TMTSF)₂X, (DMET)₂I₃ may be an ideal material in which to study them, since it does not require high pressure to stabilize a metallic phase, and spin density waves appear in magnetic fields much higher than in the TMTSF salts [28]. Also, (DMET)₂I₃ is the first organic conductor where the YAE was observed [11,29]. Interlayer resistance

$R_{zz}(\theta, \phi)$ was measured on two crystals, each measuring $\sim 0.5 \times 0.3 \times 0.15 \text{ mm}^3$, at 100 mK and 9 T by using a dilution refrigerator equipped with a two-axis (θ, ϕ) rotator. We show data for one sample, as both showed similar results.

The measured magnetoresistance is shown in Fig. 1(a), as a function of θ for various values of ϕ . Large AMRO are seen throughout. Although not shown in detail here, clear DKC oscillations, previously unreported for this material, are observed when rotating near $|\theta| = 90^\circ$ at $\phi = 0^\circ$ and 180° . LMA oscillations are also observed for θ rotations when $\phi = 90^\circ$ (dotted line). The YAE is clearly observed (again not detailed) for a ϕ rotation with fixed $|\theta| = 90^\circ$. Finally, the oscillations that appear for virtually all ϕ rotations with fixed θ are manifestations of the LN effect. Thus, *all* previously reported AMRO effects are experimentally observed in the present experiment. Next, we compare the experimental results of Fig. 1(a) with new calculations based on the actual triclinic crystal structure [Fig. 1(b)] as well as with the existing theoretical models that use an orthorhombic approximation (Fig. 2).

The magnetoconductivity tensor is calculated by solving the one-electron Boltzmann transport equation within the relaxation time approximation, using the tight binding energy dispersion $E = -2t_b \cos k_b b - 2t_a \cos k_a a -$

$2t_c \cos k_c c$, with transfer integrals along the respective lattice directions in the ratio $t_b:t_a:t_c = 300:30:1$ [30]. Once Lorentz forces and wave vectors are calculated in the Cartesian coordinate system, they are converted to the triclinic system by using an inverse matrix transformation [31]. To acquire results with sufficient precision, the first Brillouin zone is divided into a grid of $128 \times 128 \times 128$ sites. Figure 1(b) shows the resulting calculated interlayer magnetoresistivity ($\rho_c = \rho_{zz} \cong 1/\sigma_{zz}$), again as a function of θ at the same angles ϕ as for the experiment. Here, it can be seen that the calculated magnetoresistance is qualitatively and semiquantitatively in accordance with the experimental data, reproducing all known AMRO effects. The angular positions of magnetoresistance minima for various integer indices n can be defined by what can be viewed as a generalized Lebed + LN relation, which we will term LNL:

$$\tan \theta \sin \phi = n \frac{a \sin \gamma}{c \sin \alpha \sin \beta^*} + \cot \beta^*, \quad (1)$$

where the integer n is the Lebed (or LNL) index, and $\cos \beta^* = (\cos \gamma \cos \alpha - \cos \beta)/(\sin \alpha \sin \gamma)$, by using the crystal lattice angles α, β , and γ .

Figure 2 shows magnetoresistance calculations for (DMET)₂I₃ in the Lebed y - z rotation plane ($\phi = 90^\circ$). Figure 2(a) uses orthorhombic crystal symmetry (for both numerical Boltzmann and analytical Kubo formalisms [21]), while Fig. 2(b) uses the present triclinic symmetry Boltzmann model. These can be compared to our experimental data in Fig. 2(c). The positions of Lebed minima calculated from Eq. (1), by using the triclinic lattice pa-

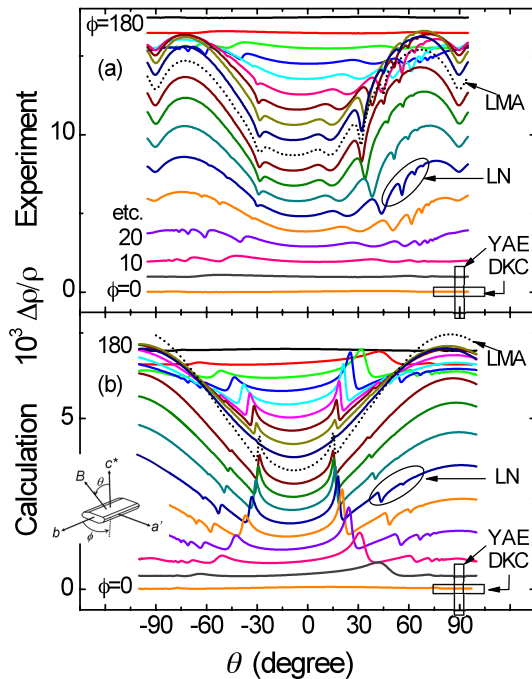


FIG. 1 (color online). (a) Interlayer magnetoresistance of (DMET)₂I₃ versus polar angle θ for different azimuthal angles ϕ at 9 T and 100 mK. (b) Calculated 9 T magnetoresistance using the triclinic crystal structure. Inset: Axis and angle definitions. As indicated, all known types of AMRO (LMA, DKC, YAE, and LN) are detected in the experiment and reproduced in the calculations (DKC and YAE are clearly evident on expanded scales). The DKC effect had not been previously reported for this compound.

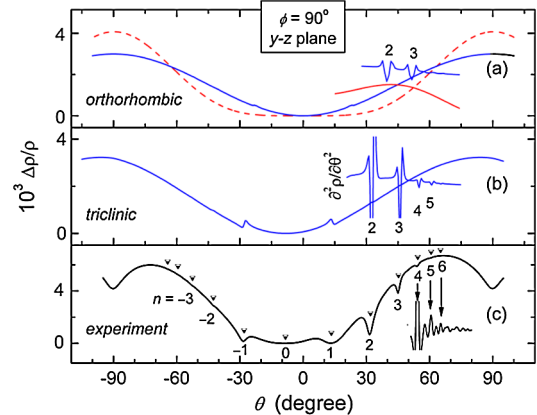


FIG. 2 (color online). Polar angle dependence (B rotated in y - z plane) of 9 T magnetoresistance: (a) orthorhombic Boltzmann numerical (solid line) and Kubo analytic (dashed line) calculations [21]; (b) present triclinic Boltzmann numerical calculation; (c) experiment. Insets show $d^2\rho/d\theta^2$, indicating the lack of Lebed oscillations in Kubo calculations and their presence in Boltzmann calculations, with triclinic symmetry yielding features ~ 10 times larger than orthorhombic. Oscillations up to $n = 5$ or higher are observed in triclinic calculations (b) and experiment (c). Triangles indicate angular positions of the resistivity minima for indices n according to Eq. (1).

rameters for $(\text{DMET})_2\text{I}_3$ [32], are in good agreement with the experimental results of Fig. 2(c). Moreover, in contrast to previous Kubo-based theoretical models [smooth solid curve with no oscillating features in Fig. 2(a)], we show that the Lebed effect appears in Boltzmann-type calculations, regardless of crystal symmetry [dashed curves with oscillating features in Figs. 2(a) and 2(c)]. In particular, our new triclinic Boltzmann calculations [Fig. 2(b)] reveal Lebed effect features on the scale shown for indices as high as $n = 5$, with oscillation amplitudes similar to the orthorhombic calculations of Fig. 1(a). Derivatives $\partial^2\rho/\partial\theta^2$ illustrate this latter point, as well as the complete absence of LMA in the Kubo model calculations [21].

There is broad agreement as well between the calculated positions of resistance minima for the generalized LNL effect, given by Eq. (1), and experimental data, as shown in Fig. 3. Here, the LNL minimum index n is plotted as a function of $\tan\theta$ for in-plane ($\phi = 90^\circ$, LMA) and out-of-plane ($\phi \neq 90^\circ$, LN) rotations. A series of symmetric patterns emerges, not about $\tan\theta = 0$ but about $\tan\theta \approx -0.15$. Moreover, these minimum positions shift progressively away from this symmetry point as rotations move away from the y-z plane (i.e., as ϕ deviates from 90°) as indicated by the curved lines. Meanwhile, the calculated index curves $n[\tan\theta]$ (straight, solid lines) are symmetric about $\tan\theta_{n=0} = -\cot\beta^* = -0.146$, owing to the triclinicity of the crystal structure [Eq. (1)]. This agrees with the above -0.15 experimental value. Figure 3 provides compelling evidence that the LMA and LN effects are in fact two aspects of the same effect, with the same underlying physics, providing rationale for the LNL moniker.

From the present calculations and experiments, it is seen that all known Q1D AMRO effects are indeed observed in $(\text{DMET})_2\text{I}_3$ and, by extension, are generic to Q1D systems with like crystal and band structures. The x-z plane DKC effect is connected directly to the details of the warped Fermi surface through the transfer integral ratio t_y/t_x [8], whereas the x-y plane YAE is ascribed to the velocity-preserving nature of “effective” electrons, via their proximity to the geometrical inflection points on the Fermi surface [13,33], which can be used to estimate the inter-plane couplings t_y and t_z . The y-z plane LMA effect, which prompted initial investigations of Q1D AMRO, can be explained in terms of the commensurability of electron trajectories across the warped Fermi surface, but the positions of the LMA magnetoresistance minima are determined only by the lattice parameters [Eq. (1)]. The more general form of LMA is the LNL effect. There appear to be, therefore, at most three distinct Q1D AMRO angular effects. The calculations do not reproduce every aspect of the measured resistivity, however. In particular, it can be seen in Figs. 1 and 2 that the measured data exhibit a broad minimum at $B \parallel y$ ($\theta = 90^\circ$), while calculations show a local maximum expected from Lorentz force considerations. While tempting to associate this behavior with

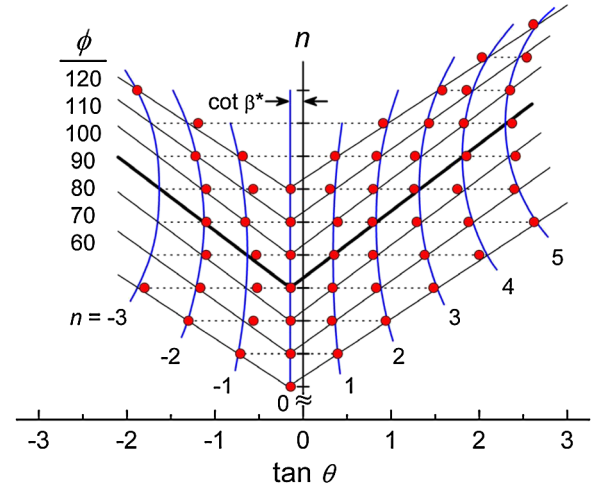


FIG. 3 (color online). Positions of experimental magnetoresistance minima (circles), indexed by n as in Fig. 2, versus $\tan\theta$ for different ϕ rotations. Solid lines are $n[\tan\theta]$ from Eq. (1) (thick line indicates Lebed plane, $\phi = 90^\circ$), showing agreement between this generalized relation and the observed LNL minima, including the angular offset $\cot\beta^*$ due to triclinicity. Data and lines for different ϕ are offset for clarity.

anomalous superconductivity for this orientation, as is seen in $(\text{TMTSF})_2\text{PF}_6$ [34], further studies will be required to address this issue.

Detailed analyses of the results of Fig. 1 reveal that the amplitudes of most LNL oscillations indeed diminish rapidly as the rotation plane approaches the LMA orientation ($\phi = 90^\circ$). Triclinic Boltzmann numerical calculations show diminishing (but finite) LNL oscillation amplitudes for all indices n while approaching the y-z plane, as shown in Fig. 4(b), while for the Kubo analytic model, all oscillations completely vanish within our calculation precision. We have also determined the amplitudes of the experimentally observed LNL features, with the results shown in Fig. 4(a). The curves in Fig. 1(a) are fit to a smooth background function ($\propto \sin^2\theta$), deviations from which are taken as oscillation amplitudes. While approximate, this procedure captures the overall dependence of the AMRO oscillations. As seen, the measured amplitudes indeed decrease, at least for $|n| > 1$, while approaching the y-z plane, where naively they were expected to be maximal. One possible explanation for this behavior, now observed in both theory and experiment, is that, as the magnetic field is tilted away from the Lebed plane, Fermi surface electrons acquire velocity components along the magnetic field which are even larger than those thought to be responsible for the original Lebed effect, resulting in stronger conductivity increases (deeper resistivity minima) for the generalized LNL effect. Likewise, detailed differences between theory and experiment may suggest that the one-electron theory employed may be too simplistic, and electron interactions, which are expected to increase in such low dimensional systems, may be involved.

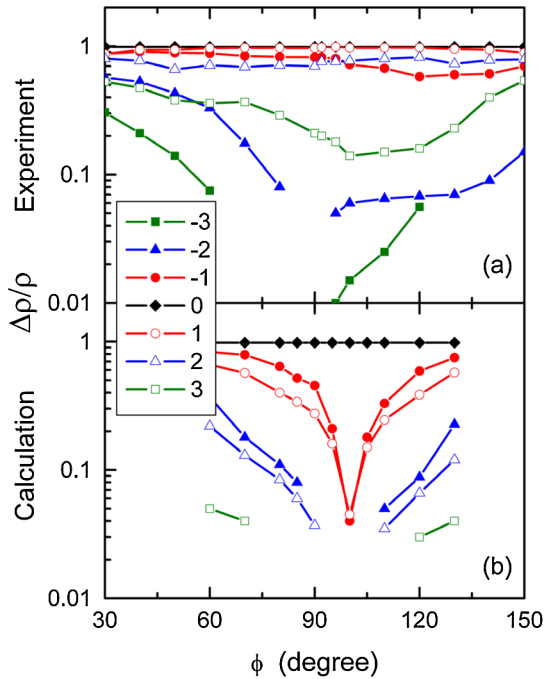


FIG. 4 (color online). Amplitudes of magnetoresistance oscillations from data and simulations in Fig. 1 for different LNL indices n versus angle ϕ as observed (a) experimentally and (b) from present triclinic calculations. High index amplitudes decrease significantly while approaching the magic angle orientation $\phi = 90^\circ$, though they remain finite.

In summary, we have measured the interlayer magnetoresistance of the Q1D molecular organic conductor (DMET)₂I₃ at low temperature and across all magnetic field orientations. All known Q1D AMRO effects are now observed in this system. We have numerically solved the interlayer magnetoconductivity tensor for the same field orientations, by using the true triclinic lattice parameters, a procedure that should now be employable for other Q1D systems. Even though the LNL amplitudes decrease while the magnetic field rotation plane approaches the y - z plane, the calculated results confirm that Lebed oscillations survive, up to at least $n = 5$ th order, in contrast to some previous theoretical models which predict their absence. These Lebed oscillations may indeed be “magic” in Q1D molecular conductors.

This work was support by the National Science Foundation, under Grant No. DMR-0605339.

- [1] T. Ishiguro, K. Yamaji, and G. Saito, *Organic Superconductors* (Springer-Verlag, Berlin, 1998), 2nd ed.
- [2] *The Physics of Organic Superconductors and Conductors*, edited by Andrei Lebed, Springer Ser. Mat. Sci. Vol. 110 (Springer, New York, 2008).

- [3] A. G. Lebed, JETP Lett. **43**, 174 (1986).
- [4] A. G. Lebed and P. Bak, Phys. Rev. Lett. **63**, 1315 (1989).
- [5] T. Osada *et al.*, Phys. Rev. Lett. **66**, 1525 (1991).
- [6] M. J. Naughton *et al.*, Phys. Rev. Lett. **67**, 3712 (1991); M. J. Naughton *et al.*, Mater. Res. Soc. Symp. Proc. **173**, 257 (1990).
- [7] W. Kang, S. T. Hannahs, and P. M. Chaikin, Phys. Rev. Lett. **69**, 2827 (1992).
- [8] G. M. Danner, W. Kang, and P. M. Chaikin, Phys. Rev. Lett. **72**, 3714 (1994).
- [9] I. J. Lee and M. J. Naughton, Phys. Rev. B **58**, R13343 (1998).
- [10] T. Osada, S. Kagoshima, and N. Miura, Phys. Rev. Lett. **77**, 5261 (1996).
- [11] H. Yoshino *et al.*, J. Phys. Soc. Jpn. **64**, 2307 (1995).
- [12] M. J. Naughton, I. J. Lee, P. M. Chaikin, and G. M. Danner, Synth. Met. **85**, 1481 (1997).
- [13] I. J. Lee and M. J. Naughton, Phys. Rev. B **57**, 7423 (1998).
- [14] H. I. Ha, A. G. Lebed, and M. J. Naughton, Phys. Rev. B **73**, 033107 (2006).
- [15] K. Maki, Phys. Rev. B **45**, R5111 (1992).
- [16] T. Osada, S. Kagoshima, and N. Miura, Phys. Rev. B **46**, 1812 (1992).
- [17] A. G. Lebed, J. Phys. I **4**, 351 (1994).
- [18] S. P. Strong, David G. Clarke, and P. W. Anderson, Phys. Rev. Lett. **73**, 1007 (1994).
- [19] R. H. McKenzie and P. Moses, Phys. Rev. Lett. **81**, 4492 (1998).
- [20] H. Yoshino and K. Murata, J. Phys. Soc. Jpn. **68**, 3027 (1999).
- [21] T. Osada, Physica (Amsterdam) **12E**, 272 (2002); T. Osada and M. Kuraguchi, Synth. Met. **133–134**, 75 (2003).
- [22] B. K. Cooper and V. M. Yakovenko, Phys. Rev. Lett. **96**, 037001 (2006).
- [23] A. G. Lebed and M. J. Naughton, Phys. Rev. Lett. **91**, 187003 (2003).
- [24] A. G. Lebed, H. I. Ha, and M. J. Naughton, Phys. Rev. B **71**, 132504 (2005).
- [25] W. Kang, T. Osada, Y. J. Jo, and H. Kang, Phys. Rev. Lett. **99**, 017002 (2007).
- [26] A. G. Lebed, N. N. Bagmet, and M. J. Naughton, Phys. Rev. Lett. **93**, 157006 (2004).
- [27] K. Kikuchi *et al.*, J. Phys. Soc. Jpn. **56**, 3436 (1987).
- [28] S. Uji *et al.*, in *Proceedings of Physical Phenomena at High Magnetic Fields III* (World Scientific, London, 1998), p. 227.
- [29] H. Yoshino *et al.*, J. Phys. Soc. Jpn. **66**, 2248 (1997).
- [30] H. Yoshino *et al.*, J. Phys. Soc. Jpn. **66**, 2410 (1997).
- [31] H. Yoshino (unpublished).
- [32] Y. Oshima *et al.*, Phys. Rev. B **68**, 054526 (2003).
- [33] A. G. Lebed and N. N. Bagmet, Phys. Rev. B **55**, R8654 (1997).
- [34] I. J. Lee, M. J. Naughton, G. M. Danner, and P. M. Chaikin, Phys. Rev. Lett. **78**, 3555 (1997).